11-2013

Optimal Control in the Treatment of Retinitis Pigmentosa

Erika T. Camacho

Luis A. Melara

Cristina Villalobos
The University of Texas Rio Grande Valley

Stephen Wirkus

Recommended Citation

Camacho, E.T., Melara, L.A., Villalobos, M.C. et al. Optimal Control in the Treatment of Retinitis Pigmentosa. Bull Math Biol 76, 292–313 (2014). https://doi.org/10.1007/s11538-013-9919-1

Please cite: Bull Math Biol (2014) 76:292–313
DOI 10.1007/s11538-013-9919-1

Optimal Control in the Treatment of Retinitis Pigmentosa

E.T. Camacho [*], L.A. Melara [†], M.C. Villalobos [‡], S. Wirkus [§]

November 1, 2012

Abstract

Numerous therapies have been implemented in an effort to minimize the debilitating effects of the degenerative eye disease Retinitis Pigmentosa (RP), yet none have provided satisfactory long-term solution. To date there is no treatment that can halt the degeneration of photoreceptors. The recent discovery of the RdCVF protein has provided researchers with a potential therapy that could slow the secondary wave of cone death. In this work, we build on an existing mathematical model of photoreceptor interactions in the presence of RP and incorporate various treatment regiments via RdCVF. Our results show that an optimal control exists for the administration of RdCVF. In addition, our numerical solutions show the experimentally observed rescue effect that the RdCVF has on the cones.

2 Background of Retinitis Pigmentosa and Photoreceptors

Retinitis pigmentosa (RP) is a heterogeneous group of diseases that affect approximately 1 in 4000 individuals with typical manifestations between adolescence and early adulthood [2, 35]. The pathogenesis of RP, while mainly genetically programmed with over 100 genes identified to dated, is a continuum of metabolic disorders leading to rod and cone photoreceptor degeneration with accompanying associated retinal pigment epithelium degeneration. The characteristics, disease progression, and age of onset of RP vary dramatically among patients, including members in the same family [2]. RP is classified by different mechanisms including genetic mutation, mode of inheritance, predominant photoreceptors involved, pattern of functional vision loss, age of onset, and others. The more common subtype of RP is rod-cone RP in which rod loss precedes the secondary degeneration of cones. Other types include cone-rod (or inverse) RP, where the cones degenerate first, and simultaneous RP, where both cell types die simultaneously. In rod-cone RP, the loss of rod cells and of their functionality at the early stages of the disease leads to poor night vision and ultimately night blindness. Because rods are located in the periphery of the retina and the cones are concentrated in the fovea (central part), the rod degeneration also leads to tunnel vision, and ultimately loss of central vision, accuity, and color vision at later stages of RP as the cones degenerate [12]. The irreparable effects of RP and its vast range of onset ranging from infancy to late adulthood make it a priority to investigate potential long term therapies and their optimal administration.

Although numerous gene mutations encoding for different proteins have been identified, it is not fully understood how these can all lead to the same common pathway of the disease. Thus, it is

[*]Assistant Professor, School of Mathematical & Natural Sciences, Arizona State University, Phoenix, AZ 85306
[†]Assistant Professor, Department of Mathematics, Shippensburg University, Shippensburg, PA, 17257
[‡]Associate Professor, Department of Mathematics, The University of Texas-Pan American, Edinburg, TX 78539
[§]Associate Professor, School of Mathematical & Natural Sciences, Arizona State University, Phoenix, AZ 85306

crucial to understand the structure and interaction of the photoreceptors (rods and cones) together with the retinal pigment epithelium (RPE) and how these specialized cells form a functional unit that is critical for sight [36]. The photoreceptors receive the incoming light photons and transmit these chemical signals to the brain through series of well-understood steps [14, 26]. In receiving light, the photoreceptors undergo a tremendous amount of stress and are equipped to continually deal with this by undergoing a periodic shedding and continuous renewal of its outer segment, which are made up of discs. The shed outer segment (OS) discs are phagocytised by the adjacent RPE. In addition, the RPE is responsible for delivering essential proteins and growth factors to the photoreceptors. In humans, a typical photoreceptor will undergo complete renewal in 9-17 days depending on its location within the retina, with a given outer segment typically shedding around 10% of its length each day [26]. In a healthy eye, new discs are continuously made (renewed) throughout the day and on average the number made equals the number shed so that the height of the photoreceptor remains roughly constant over time. In patients with RP this renewal and shedding is disturbed resulting in shorter outer segments and patchiness in certain regions indicative of photoreceptor death/absence.

Secondary Cone Wave Death and RdCVF

The secondary death of cones that often follows some six months after the complete loss of rods in rod-cone RP had puzzled researchers for many years because it occurred even when the mutations didn't directly affect the cones in most cases of RP. The mysterious secondary cone death in RP has motivated extensive experiments by researchers including mathematical investigation of the essential interactions of photoreceptors and their shedding and renewal processes [4, 5, 6, 11, 18, 19, 23, 24, 29, 30, 33, 34, 38]. The human retina reaches maturity by age five and, even though new photoreceptors are not made in mature retinas, the renewal and shedding processes are considered to be the mechanism by which photoreceptors undergo a birth and death process [3, 13, 28]. Neural degeneration of the photoreceptors that typically results from genetic defects and mutations (such as RP) are implicated in disturbances of the shedding and renewal processes resulting in abnormal photoreceptor outer segment length and thus promoting the complete disappearance of the rods and cones [24, 27]. The lack of an appropriate balance between shedding and renewal has been implicated in the progression of RP as this reflects a lack of proper photopigment movement, distribution of proteins, and functioning of the photoreceptor [5]. As apoptosis is the primary manner in which the photoreceptors die, one can also look into therapies based on preventing apoptosis [15].

Among all recent research findings, one that has gained recent popularity in terms of explaining the secondary death wave of photoreceptors in RP is the lack of the *rod-derived cone viability factor* (RdCVF). RdCVF is a truncated thioredoxin-like protein specifically expressed by photoreceptors. In 2004, Leveillard et al. discovered RdCVF and showed that this protein was necessary for the survival and functionality of cones [18]. The mathematical necessity of RdCVF for survivability of the photoreceptors was independently confirmed in [4]. Experiments revealed that the amount of RdCVF was the same in both normal and mutated rods prior to their degeneration and that any decrease in RdCVF was strongly correlated with the decrease in the number of rods during their degenerative process. In addition, the effect of RdCVF was reported to be independent of the casual mutation (autosomal-recessive or autosomal-dominant) leading to rod degeneration [38]. These investigations indicated that RdCVF had a significant cone rescuing effect; however, the protective effects of RdCVF have not been experimentally shown to extend to degenerating rods. The most important result of these investigations in terms of finding a potential long term therapy for all RP partients is that the presence of the rod cells is not necessary for cone survival as long as RdCVF is present [4, 11, 18, 19, 31, 38, 33]. The discovery of RdCVF's ability to preserve cone functionality is very promising since maintaining func-

tional cones even when 95% of the cones are gone may prevent blindness. While the identification of this protein offers new treatment possibilities for RP the mechanism by which one would effectively deliver RdCVF is still unclear [18, 33].

Treatment Options

There is no known cure for most types of RP [2]. Recently, a possible treatment that has begun to be considered is the administration of doses of RdCVF even if all the rods are gone (rod-cone RP). Besides treatment with RdCVF (still preliminary), there are few treatment options such as light avoidance and/or the use of low-vision aids to slow down the progression of RP. Researchers suggest high doses of vitamin A (15,000 IU/day) may slow progression a little in some people, but the results are not strong. More importantly, the high amount of vitamin A dosage over a prolonged time rase the risk of liver disease and thus many doctors have stopped prescribing vitamin A as a treatment of RP. Even thought recent results suggest that taking too much vitamin A can be toxic, high doses of omega-3 fatty acid (including DHA) in combination with vitamin A supplements can result in a 40% slower rate of visual acuity loss per year [1]. However, even though certain therapies (such as vitamin A and E suplementation) have shown to slow down the progression of the disease, this is not consistent with all forms of RP as some actually show an accelerated retinal degeneration due to these supplements [2]. Research has also shown that certain growth factors may help slow the progression as they are aimed at repairing or protecting damaged cells. Among these are synthetic nucleic acid nanoparticles, ciliary neurotrophic factor (CNTF), and others. Growth factors are chemicals that support cells to grow and repair themselves. Research groups are working on the potential uses of growth factors in the treatment of retinal disease in the hope that damaged cells can be repaired or protected from damage; however, delivery of these and administration is still in question [31].

Gene therapy has recently gained much attention as researchers attempt to discover ways that healthy genes can be inserted into the retina. This method relies on the gene causing the problem being known but in many cases of RP the faulty gene or genes are yet to be discovered. Once a faulty gene causing RP has been identified, gene therapy aims to replace the faulty gene within the affected retinal cells with new genes that work properly. The new genetic material, usually carried by a harmless virus, is injected directly into the affectedarea of the retina. The hope is that the cells then begin to work correctly and the damage is either stopped or reversed. The success of gene therapy in clinical trials and lab experiments is still debatable even in cases where the faulty gene is presumed to be known as results have been mixed potentially due to the variability in RP and the connectivity of the genetic vision network. Stem cell therapy is also being explored to see if stem cells injected into the retina can be persuaded to differentiate into retinal cells. Stem cells are cells that can divide (differentiate) into other cell types and they have the potential to replace damaged or missing retinal cells which is very promising since retinal cells affected by RP are very specialized cells that the body cannot replace.

Researchers have also created a retinal prosthesis, which is a man-made device intended to take over the function of the lost photoreceptors by electrically stimulating the remaining healthy cells of the retina. Through electrical stimulation, the activated ganglion cells can provide a visual signal to the brain. The visual image captured by a video camera, placed behind the affected persons glasses, is transmitted via electromagnetic radiation to a small decoder chip located on the retinal surface. Data and power are then sent to a set of electrodes connected to the decoder. Electrical current passing from individual electrodes stimulate cells in the appropriate areas of the retina corresponding to the features in the visual scene. Finally, there has been work in transplant research in which healthy retinal cells grown in the laboratory are transplanted into sick retinas. This has not yet been considered as

clinically safe and successful but some researchers believe that transplanting retinal cells with their underlying supportive RPE cell layer might be more effective. This type of treatment is still in its infancy thus it is difficult to assess the potential of this form of therapy. It is also currently not known how this treatment works. It may be via the production of growth factors by the transplanted tissue that nourishes the remaining retinal cells. Studies are assessing the transplantation of developing sheets of retinal cells grown in the laboratory.

While a myriad of treatments exist, none have shown success with all subtypes of RP. We choose to focus on the common pathway to RP (regardless of the defective gene) in the most common RP subtype— rod-cone RP. We specifically will consider treatment by administering RdCVF, which seems to be the most promising general treatment in rod-cone RP. While the understanding of RP has increased tremendously in the last two decades through physiological experimental research, a permanent therapy that will prolong the life of these photoreceptors or that will reverse its inevitable death still awaits [15, 19]. This is the catalyst behind our work in which we explore through optimal control the potential therapeutic benefits of a particular protein in human visual system.

3 Problem Formulation

In the case of RP, experimental results show that a typical disease progression involves a shortening of both types of photoreceptors before their respective deaths [32]. While different genetic defects affect specific but widely varying functional aspects of the rods, these can be thought of as "defects that affect the shedding" and "defects that affect the renewal" of the photoreceptor outer segment as they are all linked to these processes. This paper builds on previous work by Camacho et al. [4, 5] who developed mathematical models of photoreceptor interactions in a healthy eye and in a diseased eye with retinitis pigmentosa (RP). Both models incorporate the essential role that RdCVF plays in the long-term survival of the cones, as was experimentally shown by Leveillard et al. [18]. In experimental research, the administration of RdCVF to the diseased eye is currently done either with the injection of RdCVF into the eye, by expression of it from viral vectors, or by its delivery via RdCVF-producing cells [19]. In this paper, we propose an optimal control model which minimizes the dosage of the RdCVF protein that is administered to the human eye while maximizing the number of cones, that is, minimizing cone depletion. Initially, we describe the ordinary differential equations (ODE) model and then proceed to construct the optimal control problem.

3.1 ODE Model

The mathematical models in [4, 5] describe the interactions between three populations of photoreceptors (where the rods are divided into two populations based on their phenotype) and the trophic factor at time t. These populations are defined as:

- $R_n(t)$: population of normal rods,
- $R_m(t)$: population of mutated rods,
- $C(t)$: population of cones,
- $T(t)$: trophic pool (RPE).

Here we consider $R_m(t)$ to represent those rods that have begun to express the mutation and have had some aspect of their functionality compromised because of this mutation [5]. For brevity,

we drop the notation t for time, and we let $R_n \equiv R_n(t)$ and similarly for the other variables. We consider the units to be "cells." Fractions of a cell are interpreted as the photoreceptor outer segment discs and as the nutrients (such as growth factors, metabolites, ions, and water) for the trophic pool [10, 16, 20, 21, 25, 36, 37]. The system of differential equations modeling these interactions is given by

$$\begin{aligned}
\dot{R}_n &= R_n(a_n T - \mu_n - m) && (1)\\
\dot{R}_m &= R_m(a_m T - \mu_m) + mR_n && (2)\\
\dot{C} &= C(a_c T - \mu_c + d_n R_n + d_m R_m) + Cu && (3)\\
\dot{T} &= T(\Gamma - kT - \beta_n R_n - \beta_m R_m - \gamma C), && (4)
\end{aligned}$$

where the parameters are nonnegative; see Table 1 in Section 10. For simplicity, we define equations (1) - (4) as

$$\dot{\mathbf{x}} = \mathbf{f}(t, \mathbf{x}, \mathbf{u}),$$

where $\mathbf{x} = (R_n, R_m, C, T)$. In this work, we incorporate the administration of RdCVF as the term Cu in equation (3), where u is a control function of t. Experiments in [18, 19] demonstrate that including RdCVF provides a rescue effect for the cones and that the RdCVF is expresed in the neural retina but not in the RPE of the P23H rat[38]. We note that the incorporation of the term Cu does not distinguish between the current therapies involving RdCVF (the injection of it into the eye, the expression of it from viral vectors, or delivery of it by RdCVF-producing cells [19]).

3.2 Objective Functional

Since the secondary death of the cones occurs as a result of their deprivation of RdCVF, we formulate an optimal control problem that takes into account administration of RdCVF to the cones. The objective functional considers minimizing the dosage of RdCVF while maximizing cone longevity based on cell counts. The functional $u : [0, t_f] \to \mathbb{R}$ denotes the control and represents the percentage of a dosage of RdCVF administered over the time period $[0, t_f]$ that helps the cones survive. To compare our results with the qualitative results of the experiments, we consider the dosage of u administered over a period of two weeks ($t_f = 336$ hours) [18]. The optimal control problem has the state equations in (1) - (4) and objective functional

$$I(u) = \int_0^{t_f} \left(\frac{\varepsilon}{2} u(t)^2 - C \right) dt, \tag{5}$$

where the weight ε represents the importance of minimizing u. We define the set of controls U as

$$U = \{u | u \text{ is measurable}, \ 0 \le u(t) \le 1, t \in [0, t_f]\}, \tag{6}$$

which is a closed set. By the boundedness of $u(t) \in U$, the set U is convex.

4 Existence of the State Variables and Optimal Control

In this section, we prove the existence of the state variables and the optimal control $u^*(t)$. Initially, we find upper and lower bound solutions of the system (1)-(4) by excluding any terms associated with the control. In this case, the lower bound solutions of the system (1)-(4) are zero.

Now, we determine upper bounds $(R_n^{max}, R_m^{max}, C^{max}, T^{max})$ for the system (1)-(4) over the time interval $[0, t_f]$. Let the initial conditions at time $t = 0$ for the state variables be denoted by $(R_{n0}, R_{m0}, C_0, T_0)$. The upper bound solution T^{max} of (4) is given by $T^{max} = T_0 e^{\Gamma t_f}$ where $\Gamma > 0$. Using T^{max} we obtain an upper bound R_n^{max} of (1) by solving

$$\frac{dR_n}{dt} = a_n T^{max} R_n,$$

whose solution is given by $R_n(t) = R_{n0} e^{a_n T^{max} t}$ and thus an upperbound for the solution is $R_n^{max} \equiv R_{n0} e^{a_n T^{max} t_f}$. Next, we use the upperbounds T^{max} and R_n^{max} to find an upperbound solution to (2). In this case, we solve

$$\frac{dR_m}{dt} - AR_m = B$$

where $A = a_m T^{max} \geq 0$ and $B = mR_n^{max} \geq 0$. The solution is given by $R_m(t) = -\frac{B}{A} + (R_{m0} + \frac{B}{A}) e^{At}$ with upper bound

$$R_m^{max} \equiv \left(R_{m0} + \frac{B}{A} \right) e^{At_f}.$$

Finally, using T^{max} we find an upperbound solution to (3) and in a similar fashion obtain $C^{max} \equiv C_0 e^{a_c T^{max} t_f}$. We use T^{max} and C^{max} to form a set of upper bound solutions for (1)-(4). Creating new variables $(\bar{R}_n, \bar{R}_m, \bar{C}, \bar{T})$, we bound system (1)-(4) on the time interval $[0, t_f]$ as follows

$$\frac{d\bar{R}_n}{dt} = \bar{R}_n a_n T^{max} \tag{7}$$

$$\frac{d\bar{R}_m}{dt} = a_m \bar{R}_m T^{max} + m\bar{R}_n \tag{8}$$

$$\frac{d\bar{C}}{dt} = w\bar{C} + C^{max} u \tag{9}$$

$$\frac{d\bar{T}}{dt} = \Gamma \bar{T}. \tag{10}$$

where $w = a_c T^{max} + d_n R_n^{max} + d_m R_m^{max}$. In the following theorem, we use system (7)-(10) to show the existence of the state variable $\mathbf{x} = (R_n, R_m, C, T)$. Then we proceed to prove the existence of an optimal control $u^*(t)$. We use a standard procedure found in [7, 8], for example, that uses the work of Fleming and Rishel [9] (Theorem 4.1 and Corollary 4.1) to prove the existence of $u^*(t)$. Define F to be the class of functions $(\mathbf{x}, u)$ where $u \in U$ and the solution $\mathbf{x}$ of system (1)-(4) satisfies the initial conditions $(R_{n0}, R_{m0}, C_0, T_0)$.

Theorem 1 (Existence of Optimal Control) *Let* $\mathbf{x}$ *satisfy the state equations in (1)-(4) with initial conditions* $R_{n0} \equiv R_n(0)$, $R_{m0} \equiv R_m(0)$, $C_0 \equiv C(0)$ *and* $T_0 \equiv T(0)$, *let* $I(u)$ *be the objective functional defined in (5), and let* U *be given by (6). Then there exists* $u^* \in U$ *minimizing* $I(u)$

if the following conditions are met:
(a) F *is not empty.*
(b) *The admissible control set* U *is closed and convex.*
(c) *The right hand side of each of the state equations is bounded by a linear function in the control* u *and the corresponding state variable* $\mathbf{x}$*.*
(d) *The integrand of* $I(u)$ *is convex on* U *and is bounded from below by* $c_1|u|^2 - c_2$ *for some constant* $c_1 > 0$*.*

Proof: We will prove the theorem by showing that conditions (a)-(d) hold. The state system (1)-(4) has bounded coefficients and the solutions are bounded on the finite interval $[0, t_f]$ (previously shown). Therefore, by Theorem 9.2.1 from [22], a solution to the state system (1)-(4) exists. Thus F is not empty. Since U is closed and convex by definition, condition (b) is met. Each of the functions in the right hand side of (1)-(4) is continuous by definition. Define $\vec{a}(t, \mathbf{x})$ to be the right hand side of (1)-(4) excluding the control u and rewrite the function $\mathbf{f}(t, \mathbf{x}, u)$ as

$$\mathbf{f}(t, \mathbf{x}, u) = \vec{a}(t, \mathbf{x}) + C \begin{pmatrix} 0 \\ 0 \\ u \\ 0 \end{pmatrix}.$$

Rewriting $\vec{a}(t, \mathbf{x})$ as a linear transformation and applying the bounds on the solutions, we have

$$\begin{aligned} |\mathbf{f}(t, \mathbf{x}, u)| &\leq \left| \begin{pmatrix} a_n T^{max} & 0 & 0 & 0 \\ m & a_m T^{max} & 0 & 0 \\ 0 & 0 & w & 0 \\ 0 & 0 & 0 & \Gamma \end{pmatrix} \begin{pmatrix} \bar{R}_n \\ \bar{R}_m \\ \bar{C} \\ \bar{T} \end{pmatrix} \right| + C^{max} \left| \begin{pmatrix} 0 \\ 0 \\ u \\ 0 \end{pmatrix} \right| \\ &\leq D\left(|\mathbf{x}| + |\mathbf{v}|\right) \end{aligned}$$

where $\mathbf{v} = (0, 0, u, 0)$ and the constant D depends on the coefficients in the system. Therefore, $\mathbf{f}(t, \mathbf{x}, u)$ is bounded by a linear combination of the state variable $\mathbf{x}$ and the control u; this shows condition (c). For the last condition, the integrand of I is convex on U since it is a combination of linear and squared terms. Since u and C are bounded, then the integrand is bounded from below. Thus, conditions (a) - (d) have been satisfied, and Theorem 1 establishes the existence of the pair $(\mathbf{x}^*, u^*)$ which minimizes $I(u)$ over F. $\square$

5 Optimality Conditions

In this section we outline the first-order necessary optimality conditions for the optimal control problem with objective functional $I(u)$ in (5) subject to the state equations (1)-(4). The optimality conditions allow us to characterize the optimal control $u^*(t)$.

For convenience, we rewrite (5) with (1)-(4) as the following maximization problem

$$\max_u J(u) \quad \text{subject to} \quad \dot{\mathbf{x}} = \mathbf{f}(t, \mathbf{x}, u) \tag{11}$$

where

$$J(u) = -I(u) = \int_0^{t_f} \left(C - \frac{\varepsilon}{2} u^2 \right) \, dt. \tag{12}$$

Thus, we seek an optimal control u^* such that

$$J(u^*) = \max_{u \in U} J(u) \;\; \text{subject to } \dot{\mathbf{x}} = \mathbf{f}(t, \mathbf{x}, u^*).$$

Theorem 1 allows us to proceed to Pontryagin's Maximum Principle. First, we define the Hamiltonian as

$$H(\mathbf{x}, \lambda, u) = C - \frac{\varepsilon}{2} u^2 \quad + \quad \lambda^T \mathbf{f}(t, \mathbf{x}, u)$$

where $\lambda \equiv \lambda(t) = (\lambda_1(t), \lambda_2(t), \lambda_3(t), \lambda_4(t))^T$ is the vector of adjoint variables. For simplicity, we let $H \equiv H(\mathbf{x}, \lambda, u)$ and $\lambda_i \equiv \lambda_i(t)$ for $i = 1, \ldots, 4$. More explicitly, using system (1) - (4) and the objective functional in (12), the Hamiltonian is described as

$$\begin{aligned} H &= C - \frac{\varepsilon}{2} u^2 + \lambda_1 R_n (a_n T - \mu_n - m) + \lambda_2 (R_m (a_m T - \mu_m) + m R_n) \\ &+ \lambda_3 C (a_c T - \mu_c + d_n R_n + d_m R_m + u) + \lambda_4 T (\Gamma - kT - \beta_n R_n - \beta_m R_m - \gamma C). \end{aligned}$$

Theorem 2 (Pontryagin's Maximum Principle) *If u^* and $\mathbf{x}^*$ are optimal for problem (11), then there exist piecewise differentiable adjoint functions $\lambda_i : [0, t_f] \to \mathbb{R}$ for $i = 1, \ldots, 4$ such that*

$$\frac{d\lambda_1}{dt} = -\frac{\partial H}{\partial R_n} = -\lambda_1 (a_n T^* - \mu_n - m) - \lambda_2 m - \lambda_3 d_n C^* + \lambda_4 \beta_n T^* \tag{13}$$

$$\frac{d\lambda_2}{dt} = -\frac{\partial H}{\partial R_m} = -\lambda_2 (a_m T^* - \mu_m) - \lambda_3 d_m C^* + \lambda_4 \beta_m T^* \tag{14}$$

$$\frac{d\lambda_3}{dt} = -\frac{\partial H}{\partial C} = -1 - \lambda_3 (a_c T^* - \mu_c + d_n R_n^* + d_m R_m^* + u^*) + \lambda_4 \gamma T^* \tag{15}$$

$$\begin{aligned} \frac{d\lambda_4}{dt} = -\frac{\partial H}{\partial T} &= -\lambda_1 a_n R_n^* - \lambda_2 a_m R_m^* - \lambda_3 a_c C^* \\ &\quad -\lambda_4 (\Gamma - kT^* - \beta_n R_n^* - \beta_m R_m^* - \gamma C^*) + \lambda_4 k T^* \end{aligned} \tag{16}$$

with transversality conditions

$$\lambda_i(t_f) = 0, \text{ for } i = 1, 2, 3, 4.$$

In addition, the optimal control is characterized by

$$u^* = \min \left\{ 1, \left(\frac{C^* \lambda_3}{\varepsilon} \right)^+ \right\}, \tag{17}$$

where

$$r^+ = \begin{cases} r & \text{if } r \geq 0 \\ 0 & \text{if } r < 0, \end{cases}$$

with

$$r = \frac{C^*\lambda_3}{\varepsilon}.$$

We refer to (17) as the *characterization formula* for u.

We note that the optimal solution u^* depends on the adjoint variable $\lambda_3(t)$ and the state variable $C^*(t)$ which in turn depend on other adjoints and state variables and thus it is not possible to get a closed form solution of $u^*(t)$.

Applying Pontryagin's Maximum Principle, we obtain the following optimality conditions that must be met for an optimal control u^*, state variable $\mathbf{x}^*$ and adjoint function $\lambda^* : [0, t_f] \to \mathbb{R}^4$:

$$\begin{array}{lrcll} (ODE) & \dot{\mathbf{x}} & = & \nabla_\lambda H(\mathbf{x}, \lambda, u) & \equiv \quad \mathbf{f}(t, \mathbf{x}, u) \\ (ADJ) & \dot{\lambda} & = & -\nabla_{\mathbf{x}} H(\mathbf{x}, \lambda, u) & \equiv \quad g(t, \lambda, \mathbf{x}, u) \\ (M) & H(\mathbf{x}, \lambda, u) & = & \max H(\mathbf{x}, \lambda, u), & \\ (TRANS) & \lambda(t_f) & = & 0. & \end{array}$$

Note that with λ^* and with condition (M), we have $\frac{\partial H}{\partial u} = H_u = 0$ at the optimal control u^* for each t. Thus u^* is a critical point for the Hamiltonian [17]. We use this optimality condition to derive the characterization of the optimal control u^* in Section 7.

6 Description of the Discretized Variables

We approximate a solution $\mathbf{x}$ to the system (1) - (4) as described below. The time interval $[0, t_f]$ is discretized into N equally spaced subintervals with the following nodes

$$0 = t_0 < t_1 < \ldots < t_N = t_f \tag{18}$$

and

$$h = t_{i+1} - t_i, \quad \text{for} \quad i = 0, \ldots, N-1.$$

Let $\mathbf{x_k} = (R_n(t_k), R_m(t_k), C(t_k), T(t_k))^T$ be the discretized vector $\mathbf{x}$ at time t_k.
Similarly, $u_k \equiv u(t_k)$ for $k = 0, \ldots, N$. Thus the vector $\vec{u} = [u_0, u_1, u_2, \ldots, u_N]$ holds the discretized values at all time steps t_k for $k = 0, 1, \ldots, N$.

Given an initial iterate $\mathbf{x}_0 \in \mathbb{R}^4$ to the system (1) - (4) and initial control $\vec{u}$ over the time interval $[0, t_f]$, an approximation to the solution of the system (1) - (4) for state variable $\mathbf{x}$ is obtained using an implementation of a fourth-order Runge-Kutta method forward in time. Therefore, for $k = 0, \ldots, N$,

$$\begin{array}{rcl} k_1 & = & \mathbf{f}(t_k, \mathbf{x_k}, u_k) \\ k_2 & = & \mathbf{f}(t_k + \frac{h}{2}, \mathbf{x_k} + \frac{h}{2}k_1, \frac{1}{2}(u_k + u_{k+1})) \\ k_3 & = & \mathbf{f}(t_k + \frac{h}{2}, \mathbf{x_k} + \frac{h}{2}k_2, \frac{1}{2}(u_k + u_{k+1})) \\ k_4 & = & \mathbf{f}(t_{k+1}, \mathbf{x_k} + k_3, u_{k+1}) \\ \mathbf{x_{k+1}} & = & \mathbf{x_k} + \frac{h}{6}(k_1 + 2k_2 + 2k_3 + k_4). \end{array}$$

Note that in calculating k_2 and k_3 in the Runge-Kutta algorithm, u_k was replaced with the average of u_k and u_{k+1}. While there are many ways to approximate this value, approximating it with the average is sufficient [17].

To numerically compute a solution λ to the adjoint system (ADJ), we implement the Runge-Kutta algorithm backward in time. Assume the previous discretization of $[0, t_f]$ and h defined as before. Let the adjoint vector $\vec{\lambda}_k \in \mathbb{R}^4$ be defined as $\vec{\lambda}_k = (\lambda_1(t_k), \lambda_2(t_k), \lambda_3(t_k), \lambda_4(t_k))^T$ whose components are the values of the adjoint variables at discrete time t_k. We enforce the transversality condition by setting initial iterate $\vec{\lambda}_N = \vec{0}$. So, for $k = N, N-1, \ldots, 1$ we have

$$\begin{aligned}
k_1 &= g(t_k, \vec{\lambda}_k, \mathbf{x_k}, u_k) \\
k_2 &= g(t_k - \tfrac{h}{2}, \vec{\lambda}_k - \tfrac{h}{2}k_1, \tfrac{1}{2}(\mathbf{x_k} + \mathbf{x_{k-1}}), \tfrac{1}{2}(u_k + u_{k-1})) \\
k_3 &= g(t_k - \tfrac{h}{2}, \vec{\lambda}_k - \tfrac{h}{2}k_2, \tfrac{1}{2}(\mathbf{x_k} + \mathbf{x_{k-1}}), \tfrac{1}{2}(u_k + u_{k-1})) \\
k_4 &= g(t_{k-1}, \vec{\lambda}_k - k_3, \mathbf{x_{k-1}}, u_{k-1}) \\
\vec{\lambda}_{k-1} &= \vec{\lambda}_k - \tfrac{h}{6}(k_1 + 2k_2 + 2k_3 + k_4).
\end{aligned}$$

7 Updating the Control Variable

In this section, we derive the characterization of the optimal control. By Pontryagin's Maximum Principle, at optimality the Hamiltonian satisfies

$$\frac{\partial H}{\partial u} = 0 = -\varepsilon u + C\lambda_3. \tag{19}$$

Then the optimal control u^* is

$$u^* = \min\left\{1, \left(\frac{C^*\,\lambda_3}{\varepsilon}\right)^+\right\},$$

where the notation for $(C^*\,\lambda_3/\varepsilon)^+$ is defined in (17).

At the discrete time t_k, we compute the discrete characterization of u^* using (17), which we denote as $u1_k = u1(t_k)$. Therefore, we have

$$u1_k = \min\left(1, \left(\frac{C(t_k)\,\lambda_3(t_k)}{\varepsilon}\right)^+\right) \text{ for each } k. \tag{20}$$

Then the update for u_{k+1} is computed by taking the average of $u1_k$ and u_k (see [17]) as follows:

$$u_{k+1} = \frac{u1_k + u_k}{2} \text{ for } k = 0, 1, \ldots, N-1.$$

Once these values have been obtained over the discretized time interval $[0, t_f]$, we form the new vector $\vec{u} = [u_0, u_1, u_2, \ldots, u_N]$ of control variables to test convergence.

8 Convergence

Consider the discretization of $[0, t_f]$ given in (18). Let $\vec{u} \equiv \vec{u}(t) \in \mathbb{R}^{N+1}$ to be the discretization of u over $[0, t_f]$ where

$$\vec{u} = (u(t_0), u(t_1), u(t_2), \ldots, u(t_f)),$$

contains the estimated values from the current run of the Forward-Backward Sweep Method (FBSM). Define $\vec{u}_{old} \in \mathbb{R}^{N+1}$ to contain values of u from the previous run of FBSM.

A stopping criteria for the control $\vec{u}$ requires the relative error to be less than tolerance δ, namely,

$$\frac{\|\vec{u} - \vec{u}_{old}\|}{\|\vec{u}\|} \leq \delta$$

where $\|\cdot\|$ denotes the ℓ_1 vector norm [17]. The above inequality is rewritten as

$$\delta\|\vec{u}\| - \|\vec{u} - \vec{u}_{old}\| \geq 0 \tag{21}$$

to allow for controls that take value zero. Following [17], we define β_1 to be

$$\beta_1 \quad = \quad \delta\|\vec{u}\| - \|\vec{u} - \vec{u}_{old}\|.$$

Similarly, we use the same stopping criteria for each of the estimated state variables $\mathbf{x} = (\mathbf{x}_1(t), \mathbf{x}_2(t), \mathbf{x}_3(t), \mathbf{x}_4(t)) \in \mathbb{R}^{4\times N+1}$, obtained from the current run of the FBSM. Therefore, $\mathbf{x}$ contains the estimated values over the interval $[0, t_f]$ and is given by

$$\mathbf{x} = \begin{pmatrix} x_1(t_0) & x_1(t_1) & x_1(t_2) & \cdots & x_1(t_f) \\ x_2(t_0) & x_2(t_1) & x_2(t_2) & \cdots & x_2(t_f) \\ x_3(t_0) & x_3(t_1) & x_3(t_2) & \cdots & x_3(t_f) \\ x_4(t_0) & x_4(t_1) & x_4(t_2) & \cdots & x_4(t_f) \end{pmatrix}.$$

The estimated state variables from the previous run of FBSM are stored in the vector $\mathbf{x_{old}} \in \mathbb{R}^{4\times N+1}$. Again, we define

$$\beta_{i+1} = \delta\|\mathbf{x}_i\| - \|\mathbf{x}_i - \mathbf{x}_{old_i}\|,\ i = 1, \ldots, 4.$$

The same stopping criteria is applied to the adjoint variables. The matrix $\vec{\lambda} = (\vec{\lambda}_1(t), \vec{\lambda}_2(t), \vec{\lambda}_3(t), \vec{\lambda}_4(t)) \in \mathbb{R}^{4\times N+1}$ contains the estimated values of adjoint variables over $[0, t_f]$ which were obtained from the current run of FBSM. The matrix $\vec{\lambda}_{old} \in \mathbb{R}^{4\times N+1}$ contains the estimated values from the previous run of FBSM. Once again, we define,

$$\beta_{i+1} = \delta\|\vec{\lambda}_i\| - \|\vec{\lambda}_i - \vec{\lambda}_{old_i}\|,\ i = 5, \ldots, 8.$$

This results in the following set

$$\{\beta_1, \beta_2, \ldots, \beta_9\}.$$

If

$$\min\{\beta_1, \beta_2, \beta_3, \ldots, \beta_9\} > 0,$$

then convergence has been obtained. Otherwise, we perform another run of FBSM and continue with the same procedure.

9 Algorithm

The following algorithm summarizes the numerical approximation to the solution of (11). Given uniform discretization of the time interval $[0, t_f]$ with mesh size h, stopping criteria $\delta > 0$ and initial condition $\mathbf{x}(t_0)$.

1. Initialize $\vec{u} = 0$.
2. Use $\vec{u}$ and $\mathbf{x}(t_0)$ to approximate solution $\mathbf{x}$ to (ODE) forward in time t over $[0, t_f]$.
3. Use $\vec{\lambda}(t_f) = 0$, $\mathbf{x}$, and $\vec{u}$ to approximate solution $\vec{\lambda}$ to (ADJ) backward in time t over $[0, t_f]$.
4. Update $\vec{u}$ using the characterization formula (17).
5. Test for convergence. If convergence fails, return to Step 2 using the updated values for $\mathbf{x}$ and $\vec{u}$ and repeat.

We define a single completion of steps 2 - 5 as one iteration.

10 Numerical Results and Discussion

We present numerical results depicting five different stages of rod and cone decay. Normal levels of rods and cones in the human eye are 90-120 million and 4.5-6 million, respectively. The number of rods includes both normal and mutated rods. The trophic factor consists of many biological components and is not quantified as a unit, [4]. The trophic pool is mediated by the RPE and thus it is also in the millions. Each of the initial conditions correspond to a stage and the optimal control problem is solved for each stage to study the rescue effects of the cones under the various circumstances. In an effort to isolate the effect of RdCVF, we assume that the trophic pool is not affected in the initial three stages and it is minimally affected in the last two stages. Table 1 shows the different stages with the corresponding initial conditions given in millions for rods, cones and trophic factor.

The units of time t are days and $t \in [0, 14]$, see [18]. The stopping criteria is $\delta = 1 \times 10^{-3}$. Table 2 shows the values of parameters for the state equations (1)-(4). These parameter values were obtained from [5]. The percent of rescue effect is computed using the following formula

$$\%\text{ rescue effect } = \frac{C(t_f) - \hat{C}(t_f)}{|C(t_f) - C(t_0)|}$$

where function values $C(t_0)$ and $C(t_f)$ are the initial and final number of cones without treatment, respectively. The function value $\hat{C}(t_f)$ represents the final number of cones after treatment.

Table 1: Table of initial conditions for five stages

initial conditions	STAGE 1	STAGE 2	STAGE 3	STAGE 4	STAGE 5
$R_n(0)$	9.2×10^7	1.0×10^7	0	0	0
$R_m(0)$	2.0×10^6	7.3×10^7	3.0×10^6	0	0
$C(0)$	4.5×10^6	4.4×10^6	4.1×10^6	3.7×10^6	7.0×10^5
$T(0)$	2.34×10^6	2.34×10^6	2.34×10^6	2.32×10^6	2.25×10^6

The weight $\varepsilon > 0$ from (12) represents the importance of minimizing the control function u. For large ε, the control u is close to 0. Similarly, for small ε, the control function u is close to 1. Table 3 gives a summary of the rescue effect at each stage for various values of ε in order to produce approximately 40% rescue effect of cones in Stage 5 [5, 18, 38]. Stages 4 and 5 represent the situations in which all rods have died and thus the only source of RdCVF in cones is from administration of it.

Due to the magnitudes of the parameter values in Table 2, the numerical implementation used nondimensionalized state equations of (1)-(4). The time variable t and the control function u were not rescaled.

Table 2: Table of parameter values

parameter	value	description
a_n	4.5×10^{-8}	renewal rate of R_n outer segments mediated by T
a_m	*varies*	renewal rate of R_m outer segments mediated by T
a_c	*varies*	renewal rate of C outer segments mediated by T
k	*varies*	limiting capacity of trophic factors
d_m	1.3×10^{-11}	direct help of RdCVF given to cones by mutated rods
d_n	1.29×10^{-11}	direct help of RdCVF given to cones by normal rods
m	3.68×10^{-7}	mutation rate of normal rods
β_n	1×10^{-9}	rate of trophic pool usage by normal rods
β_m	1×10^{-9}	rate of trophic pool usage by mutated rods
μ_c	$1/9$	shedding rate of cones
μ_m	$1/9.5$	shedding rate of mutated rods
μ_n	$1/9.5$	shedding rate of normal rods
γ	4.88×10^{-8}	rate of trophic pool usage by cones
Γ	1.48	total inflow rate into the trophic pool

Table 3: Percentage of cone rescue effect and number of iterations. Decreasing the value of ε corresponds to higher dosages of the treatment administered.

DESCRIPTION	STAGE 1	STAGE 2	STAGE 3	STAGE 4	STAGE 5
ε	1.0×10^{13}	5.0×10^{12}	1.0×10^{12}	4.0×10^{9}	1.8×10^{9}
Rescue effect	1.21%	0.71%	9.01%	40.24%	40.59%
Iterations	10	10	10	12	11

Experimental evidence suggests that RdCVF has little to no effect on degenerating rods and that the rescue effect of RdCVF on cones increases with a higher concentration in the absence of rods [18]. The numerical results in Figures 1 and 2, associated with the early stages of RP, show some portion of normal rods are still present and some fraction of rods have had their functionality affected by the expresssion of the mutated gene and are thus now considered as mutated rods. As expected, the normal rods population dereases and the mutated rod population also decreases but at a slower rate over time in Stages 1 and 2. As we are focusing on the common pathway to photoreceptor degeneration, we see that the cone population is relatively unaffected (but with a slight decrease) likely due to less availability of RdCVF from rods. This effect is balanced with a greater availability of trophic factors since rods are now far fewer in number. One might expect this very early in the disease but only for a short time while reactive oxidative species and other negative side effects lead to depletion of the RPE (trophic pool). The Stage 3 graph of Figure 3 demonstrates this similar situation but when all of the normal rods have disappeared. The effect is magnified in comparison with the Stage 1 and 2 results.

Administration of RdCVF to replace that lost by the degenerating rods is shown to have a 40% rescue affect on the cone population [18, 38]. Choosing ϵ values as shown in Table 3 shows that we can find the dosage of RdCVF that will give this observed 40% rescue effect. Stage 4 shows the beginning of the secondary cone loss whereas Stage 5 shows a situation in which nearly all cones have disappeared. Stage 5 is particularly significant because experimental research suggests that day vision still occurs when only 5% of the cones are still present. Thus it is crucial to consider these two late stage scenarios in which both normal and mutated rods have completely degenerated. Such an individual will experience night blindness together with tunnel vision during the day with some accuity loss. In both Figure 4 and Figure 5, cone degeneration is slowed down through the administration of RdCVF even after all rods have disappeared. Table 3 summarizes the percentage of the cone rescue effect and the number of iterations computed to obtain convergence. The numerical results in Figures 1 - 5 also show that the number of rods were unaffected by the treatment in all five stages and the trophic factor stays roughly constant.

As treatment of rod-cone RP with RdCVF in order to prevent the secondary cone loss is being examined experimentally, it is crucial to have a better understanding of how this treatment affects our system. Equally important is to have an idea of the amount of dosage necesary to halt the progression of complete vision loss as some high dosage may lead to a reverse effect of other dangerous side effects such as the case with high prolonged dosages of vitamin A. We have shown that the mathematical modeling of photoreceptor interaction with administration of RdCVF has a rescue effect on the cones that is observed experimentally. Once researchers have a better understanding of any toxicity or other potential secondary issues associated with large dosages of RdCVF, this model can be used to guide levels of administration of this essential protein. The results of this model suggest that the combined

earlier mention of vitamin A therapy and omega 3 therapy together with administration of RdCVF may be the best way to slow the deneration of the photoreceptors. The former can help sustain the RPE or minimize its decay by assisting it in dealing with all the metabolic demands while the latter can help maintain the remaining cones without further demain on the RPE and possibly prevent the complete loss of cones, thereby preserving some day vision.

Please cite: Bull Math Biol (2014) 76:292–313
DOI 10.1007/s11538-013-9919-1

References

[1] Eliot L. Berson. Retinal photorecptor-pigment epithelium interactions: Friedenwald lecture. Investigative Ophthalmology and Visual Science, pages 1659–1676, April 1993.

[2] Dean Besharse, Josephand Bok. The Retina and Its Disorders. Academic Press, 2011.

[3] Dean Bok. Retinal photorecptor-pigment epithelium interactions: Friedenwald lecture. Investigative Ophthalmology and Visual Science, December 1985.

[4] Erika T. Camacho, Miguel A. Colón Vélez, Daniel J. Hernández, Ubaldo Rodríguez Bernier, Jon van Laarhoven, and Stephen Wirkus. A mathematical model for photoreceptor interactions. Journal of Theoretical Biology, 21:638–646, 2010.

[5] Erika T. Camacho and Stephen Wirkus. Tracing the progression of retinitis pigmentosa via photoreceptor interactions. Journal of Theoretical Biology, 317C:105–118, 2013.

[6] Miguel A. Colón Vélez, Daniel J. Hernández, Ubaldo Rodríguez Bernier, Jon van Laarhoven, and Erika T. Camacho. A mathematical model of photoreceptor interactions. Department of Biological Statistics and Computational Biology Technical Report BU-1640-M, Cornell University, 2003. 25-69.

[7] L.G. DePillis, K.R. Fister, W. Gu, T. Head, K. Maples, A. Murugan, T. Neal, and K. Yoshida. Chemotherapy for tumors: An analysis of the dynamics and a study of quadratic an linear optimal controls. Mathematical Biosciences, 209:292–315, 2007.

[8] L.G. DePillis, K.R. Fister, W. Gu, T. Head, K. Maples, T. Neal, A. Murugan, and K. Kozai. Optimal control of mixed immunotherapy and chemotherapy of tumors. Journal of Biological Systems, 16(1):51–80, 2008.

[9] W.H. Fleming and R.W. Rishel. Deterministic and stochastic optimal control. Springer-Verlag, New York, 1975.

[10] Maria Frasson, Serge Picaud, Theirry Léveillard, Manuel Simonutti, Saddek Mohand-Saïd, Henri Dreyfus, David Hicks, and José Sahel. Glial cell line-derived neurotrophic factor induces histologic and functional protection of rod photoreceptors in the rd/rd mouse. Invest Ophthalmol Vis Sci, 40:844–856, 1999.

[11] Sylavin Hanein, Isabelle Perrault, Sylvie Gerber, Hélène Dollfus, Jean-Louis Dufier, Josué Feingold, Arnold Munnich, Shomi Bhattacharya, Josseline Kaplan, José-Alain Sahel, Jean-Michel Rozet, and Thierry Leveillard. Retinal Degenerative Diseases, chapter Disease-associated variants of the Rod-derived Cone Viability Factor (RdCVF) in Leber Congenital Amaurosis. Springer, 2006. 9-14.

[12] Dyonne T. Hartong, Eliot L. Berson, and Thaddeus P. Dryja. Retinitis pigmentosa. The Lancet, 368:1795–809, 2006.

[13] Anita Hendrickson, Keely Bumsted-O'Brien, Riccardo Natoli, Visvanathan Ramamurthy, Daniel Possing, and Jan Provis. Rod photoreceptor differentiation in fetal and infant human retina. Experimental Eye Research, 87:415–426, 2008.

[14] James Keener and James Sneyd. Mathematical Physiology II: Systems Physiology. Springer, 2008.

[15] Fiona Kernan, Alex G. McKee, G. Jane Farrar, and Peter Humphries. Ophthalmology Research: Retinal Degenerations: Biology, Diagnostics, and Therapeutics, chapter On The Suppression of Photoreceptor Cell Death in Retinitis Pigmentosa. Humana Press Inc., 2007.

[16] Matthew M. LaVail, Douglas Yasumura, Michael T. Matthes, Cathy Lau-Villacorta, Kazuhiko Unoki, Ching-Hwa Sung, and Roy H. Steinberg. Protection of mouse photoreceptors by survival factors in retinal degenerations. Investigative Ophthalmology and Visual Science, 39:592–602, 1998.

[17] S. Lenhart and J.T. Workman. Optimal Control Applied to Biological Models. Chapman & Hall/CRC Mathematical and Computational Biology Series, 2007.

[18] Theirry Léveillard, Saddek Mohand-Saïd, Olivier Lorentz, David Hicks, Anne-Claire Fintz, Emmanuelle Clérin, Manuel Simonutti, Valérie Forster, Nükhet Cavusoglu, Frédéric Chalmel, Pascal Dollé, Olivier Poch, George Lambrou, and José Alain Sahel. Identification and characterization of rod-derived cone viability factor. Nature Genetics, 36(7), 2004.

[19] Theirry Léveillard and José-Alain Sahel. Rod-derived cone viability factor for treating blinding diseases: From clinic to redox signaling. Degenerative Retinal Disorders, 2:1–13, 2010.

[20] Yiwen Li, Weng Tao, Lingyu Luo, Deqiang Huang, Konrad Kauper, Paul Stabila, Matthew M. LaVail, Alan M. Laties, and Rong Wen. Cntf induces regeneration of cone outer segments in a rat model of retinal degeneration. PLoS ONE, 5:1–7, 2010.

[21] Rebecca Longbottom, Marcus Fruttigera, Ron H. Douglasb, Juan Pedro Martinez-Barberac, John Greenwooda, and Stephen E. Mossa. Genetic ablation of retinal pigment epithelial cells reveals the adaptive response of the epithelium and impact on photoreceptors. Proc. Natl Acad. Sci., 3:18728–18733, 2009.

[22] D.L. Lukes. Differential Equations: Classical to Controlled. Academic Press, 1982.

[23] Katherine M. Malanson and Janis Lem. Progress in Molecular Biology and Translational Science, chapter Rhodopsin-Mediated Retinitis Pigmentosa. Elsevier, 2009. 1-31.

[24] Saddek Mohand-Said, David Hicks, Theirry Léveillard, Serge Picaud, Fernanda Porto, and José A. Sahel. Rod-cone interactions: Developmental and clinical significance. Progress in Retinal and Eye Research, 20(4):451–467, 2001.

[25] Yusuke Murakami, Yasuhiro Ikeda, Yoshikazu Yonemitsu, Mitsuho Onimaru, Kazunori Nakagawa, Ri-ichiro Kohno, Masanori Miyazaki, Toshio Hisatomi, Makoto Nakamura, Takeshi Yabe, Mamoru Hasegawa, Tatsuro Ishibashi, and Katsuo Sueishi. Inhibition of nuclear translocation of apoptosis-inducing factor is an essential mechanism of the neuroprotective activity of pigment epithelium-derived factor in a rat model of retinal degeneration. The American Journal of Pathology, 173:1326–1338, 2008.

[26] Clyde W. Oyster. The Human Eye: Structure and Function. Sinauer Associates, Inc., 1999.

[27] Aristofanis Pallikaris, David R. Williams, and Heidi Hofer. The reflectance of single cones in the living human eye. Investigative Ophthalmology and Visual Science, 44:10, 2003.

[28] David S. Papermaster. The birth and death of photoreceptors: The friedenwald lecture. Investigative Ophthalmology and Visual Science, 43(5), May 2002.

[29] James K. Phelan and Dean Bok. A brief review of retinitis pigmentosa and the identified retinitis pigmentosa genes. Molecular Vision, 6:116–124, 2000.

[30] Claudio Punzo, Karl Kornacker, and Constance L Cepko. Stimulation of the insulin/mtor pathway delays cone death in a mouse model of retinitis pigmentosa. Nature Neuroscience, 12(1), Jan 2009.

[31] Sacha Reichman, Ravi Kiran Reddy Kalathur, Sophie Lambard, Najate Aït-Ali1, Yanjiang Yang, Aurélie Lardenois, Raymond Ripp, Olivier Poch, Donald J. Zack, José-Alain Sahel, and Thierry Léveillard. The homeobox gene chx10/vsx2 regulates rdcvf promoter activity in the inner retina. Human Molecular Genetics, 19:250–261, 2010.

[32] H. Ripps, K.P. Brin, and R.A. Weale. Rhodopsin and visual threshold in retinitis pigmentosa. Invest. Ophthalmol. Visual Sci, 17:735–745, 1978.

[33] Jose-Alain Sahel. Saving cone cells in hereditary rod diseases: A possible role for rod-derived cone viability factor (rdcvf) therapy. Retina, the Journal of Retinal and Vitreous Diseases, Supplement, 25(8):S38–39, 2005.

[34] Jikui Shen, Xiaoru Yang, Aling Dong, Robert M. Petters, You-Wei Peng, Fulton Wong, and Peter A. Campochiaro. Oxidative damage is a potential cause of cone cell death in retinitis pigmentosa. Journal of Cellular Physiology, 203:457–464, 2005.

[35] Kelly Shintani, Diana L. Shechtman, and Andrew S. Gurwood. Review and update: Current treatment trends for patients with retinitis pigmentosa. Optometry, 80:384–401, 2009.

[36] Olaf Strauss. The retinal pigment epithelium in visual function. Physiol. Rev, 85:845–881, 2005.

[37] Andreas Wenzel, Christian Grimm, Marijana Samardzija, and Charlotte E. Remé. Molecular mechanisms of light-induced photoreceptor apoptosis and neuroprotection for retinal degeneration. Progress in Retinal and Eye Research, 24:275–373, 2005.

[38] Ying Yang, Saddek Mohand-Said, Aude Danan, Manuel Simonutti, Valerie Fontaine, Emmanuelle Clerin, Serge Picaud, Thierry Léveillard, and José-Alain Sahel. Functional cone rescue by rdcvf protein in a dominant model of retinitis pigmentosas. Molecular Therapy, 17:787–795, 2009.

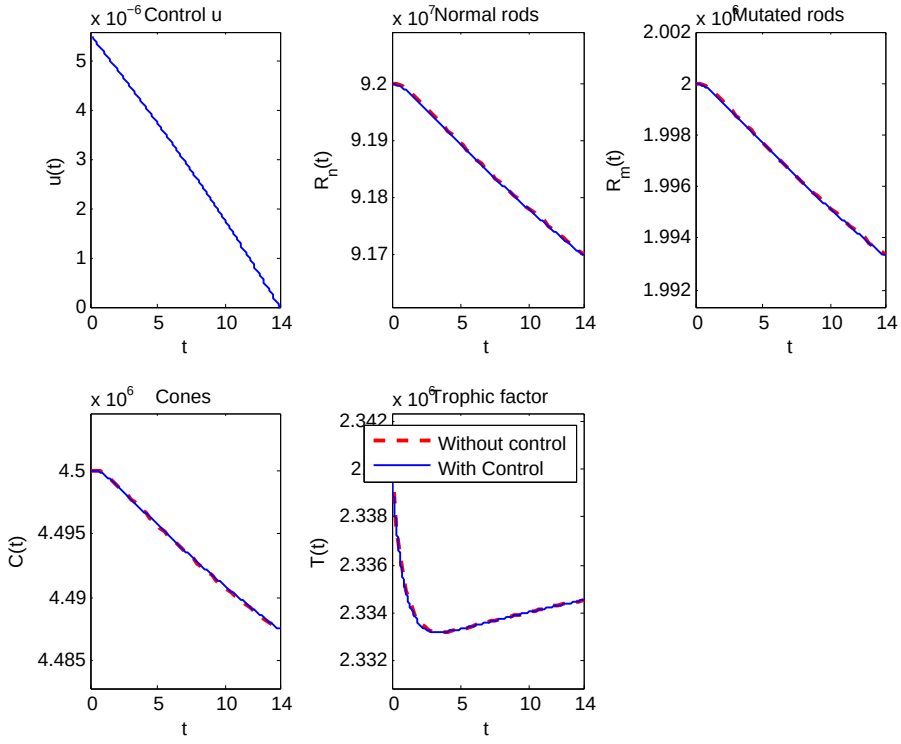

Figure 1: **Stage 1: IC** $(R_n, R_m, C, T) = (9.2\times10^7,\ 2.0\times10^6,\ 4.5\times10^6,\ 2.34\times10^6)$**. This represents an early stage of RP in which most of the normal rods are still present and only a small fraction of rods have had their functionality affected by the expresssion of the mutated gene. Over time, the normal rods population dereases as the mutated rod population also decreases but at a slower rate. The cone population also decreases for a time, likely due to less availability of RdCVF from rods but this is also offset somewhat by the greater availability of trophic factors (due to less rods). The following parameter values were used** $a_m = 4.501\times10^{-8}, a_c = 4.71\times10^{-8}$ **and** $k = 5\times10^{-7}$**. Top left:** Control u vs. time t. **Top middle:** Normal rods vs. time. **Top right:** Mutated rods vs. time. **Bottom left:** Cones vs. time. **Bottom right:** Rod-trophic factor vs. time.

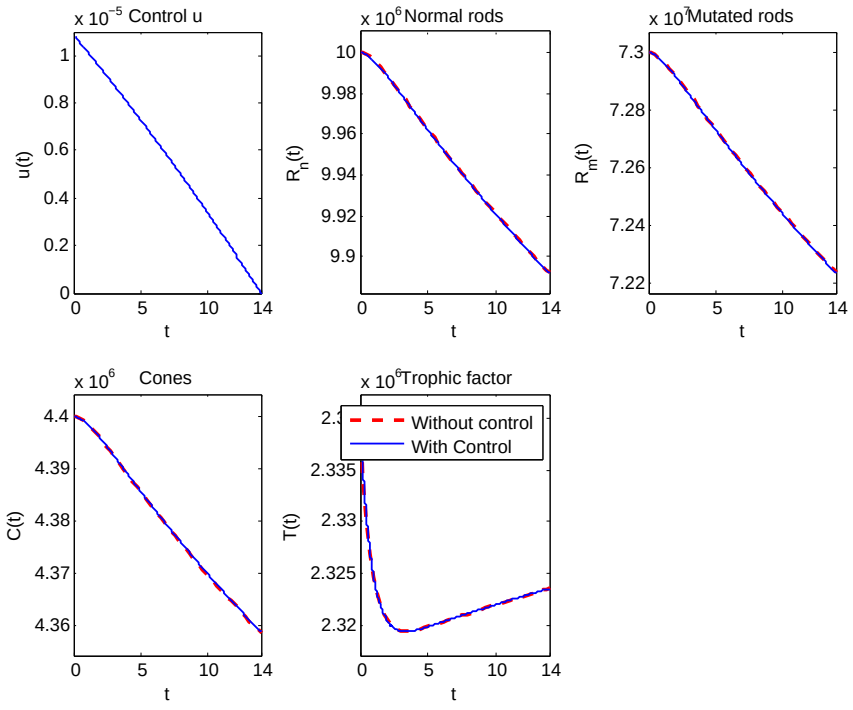

Figure 2: **Stage 2 IC** $(R_n, R_m, C, T) = (1.0 \times 10^7,\ 7.3 \times 10^7,\ 4.4 \times 10^6,\ 2.34 \times 10^6)$**. This represents a stage of RP in which most of the normal rods have disappeared although some are still present and the mutated rod population is the larger of the two. Over time, both the normal and mutated rod populations again decrease. The cone population also decreases for a time, likely due to less availability of RdCVF from rods but this is also offset somewhat by the greater availability of trophic factors (due to less rods). The following parameter values were used** $a_m = 4.501 \times 10^{-8}, a_c = 4.71 \times 10^{-8}$ **and** $k = 5 \times 10^{-7}$**. Top left:** Control u vs. time t. **Top middle:** Normal rods vs. time. **Top right:** Mutated rods vs. time. **Bottom left:** Cones vs. time. **Bottom right:** Rod-trophic factor vs. time.

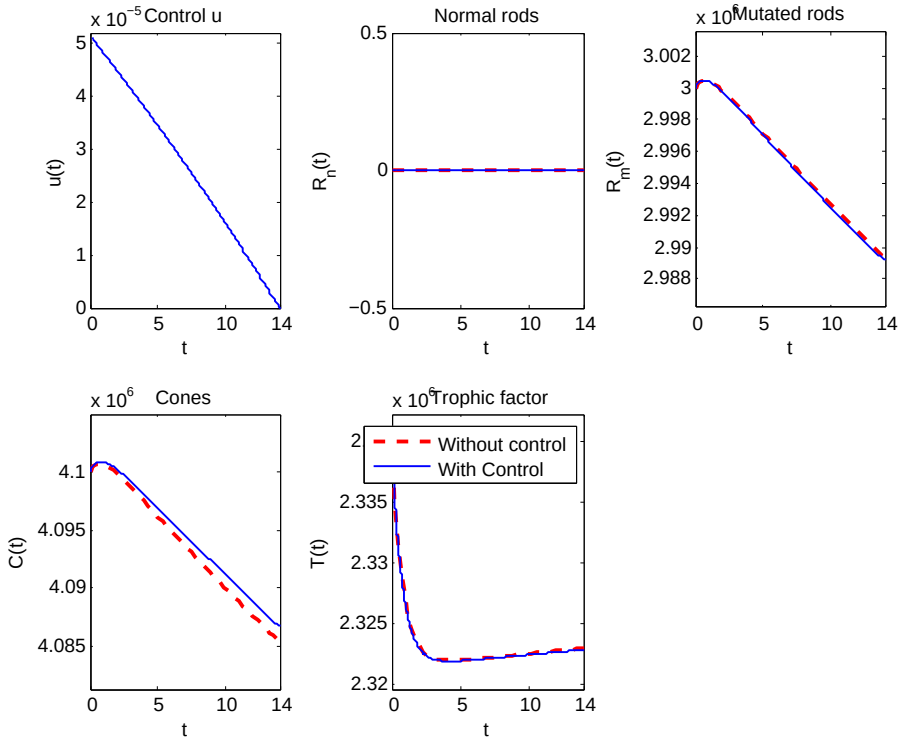

Figure 3: **Stage 3: IC** $(R_n, R_m, C, T) = (0,\ 3.0 \times 10^6,\ 4.1 \times 10^6,\ 2.34 \times 10^6)$**. This represents a middle stage of RP in which all the normal rods have disappeared with some mutated rods still present. The mutated rod population and cone population decrease as a result of RP and of less availability of RdCVF, respectively. We see some effect when the control is realized. The following parameter values were used** $a_m = 4.52 \times 10^{-8}, a_c = 4.77 \times 10^{-8}$ **and** $k = 5.5 \times 10^{-7}$**. Top left:** Control u vs. time t. **Top middle:** Normal rods vs. time. **Top right:** Mutated rods vs. time. **Bottom left:** Cones vs. time. **Bottom right:** Rod-trophic factor vs. time.

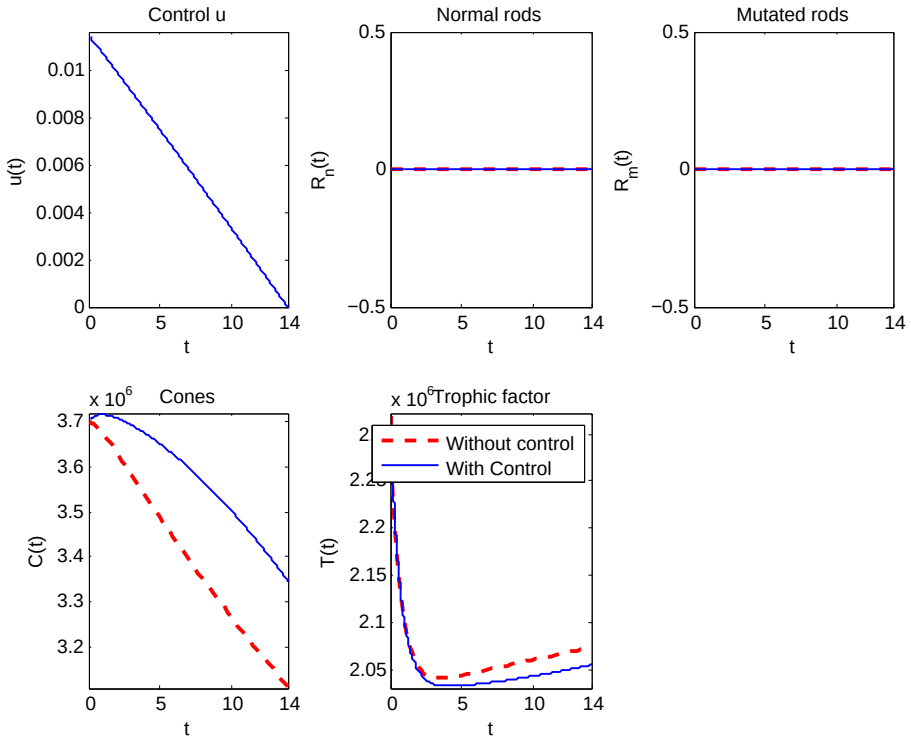

Figure 4: **Stage 4: IC** $(R_n, R_m, C, T) = (0,\ 0,\ 3.7 \times 10^6,\ 2.32 \times 10^6)$**. This represents a late stage of RP in which both rod populations have completely died off. Without RdCVF, the cone population would die off but the administration via the control shows a rescuing effect of the cone population at the level of 40%. The following parameter values were used** $a_m = 4.52 \times 10^{-8}, a_c = 4.78 \times 10^{-8}$ **and** $k = 6.4 \times 10^{-7}$**. Top left:** Control u vs. time t. **Top middle:** Normal rods vs. time. **Top right:** Mutated rods vs. time. **Bottom left:** Cones vs. time. **Bottom right:** Rod-trophic factor vs. time.

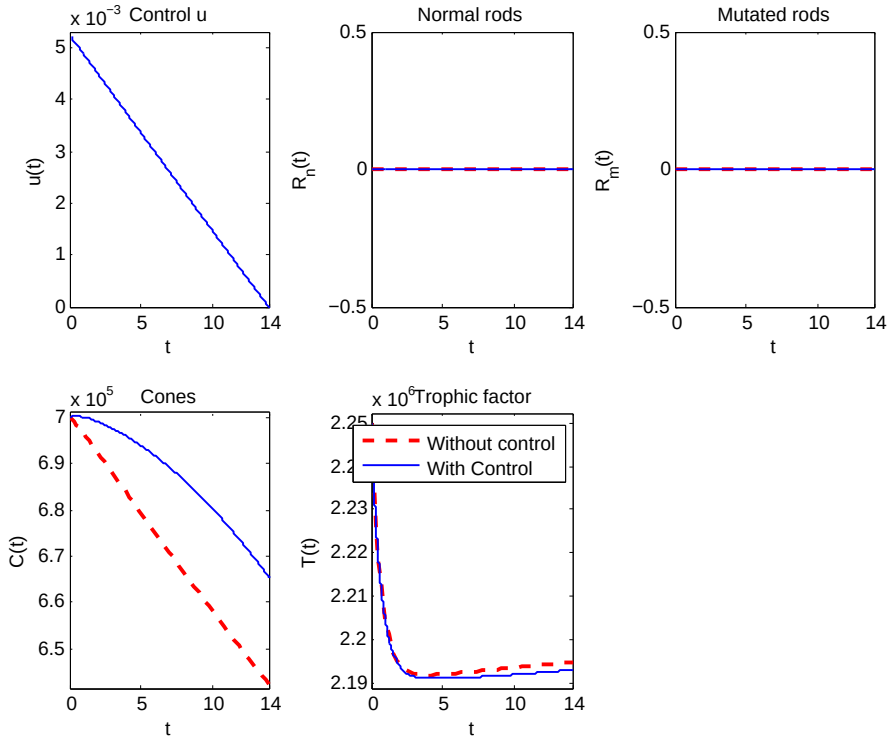

Figure 5: **Stage 5: IC** $(R_n, R_m, C, T) = (0,\ 0,\ 7.0 \times 10^5,\ 2.25 \times 10^6)$**. This represents a very late stage of RP in which both rod populations have completely died off and the cone population is near extinction too. Without RdCVF, the cone population would die off but the administration via the control again shows a rescuing effect of the cone population at the level of 40%. The following parameter values were used** $a_m = 4.52 \times 10^{-8}, a_c = 4.78 \times 10^{-8}$ **and** $k = 6.6 \times 10^{-7}$**. Top left:** Control u vs. time t. **Top middle:** Normal rods vs. time. **Top right:** Mutated rods vs. time. **Bottom left:** Cones vs. time. **Bottom right:** Rod-trophic factor vs. time.

Please cite:Bull Math Biol (2014) 76:292–313
DOI 10.1007/s11538-013-9919-1